

**Recurrence-plot-based measures of complexity and their application to heart-rate-variability data**Norbert Marwan,<sup>1\*</sup> Niels Wessel,<sup>1</sup> Udo Meyerfeldt,<sup>2</sup> Alexander Schirdewan,<sup>2</sup> and Jürgen Kurths<sup>1</sup><sup>1</sup>*Nonlinear Dynamics Group, Institute of Physics, University of Potsdam, Potsdam 14415, Germany*<sup>2</sup>*Franz-Volhard-Hospital, HELIOS Kliniken Berlin, Charité, Humboldt University Berlin, Wiltbergstrasse 50, 13125 Berlin, Germany*

(Received 7 January 2002; published 6 August 2002)

The knowledge of transitions between regular, laminar or chaotic behaviors is essential to understand the underlying mechanisms behind complex systems. While several linear approaches are often insufficient to describe such processes, there are several nonlinear methods that, however, require rather long time observations. To overcome these difficulties, we propose measures of complexity based on vertical structures in recurrence plots and apply them to the logistic map as well as to heart-rate-variability data. For the logistic map these measures enable us not only to detect transitions between chaotic and periodic states, but also to identify laminar states, i.e., chaos-chaos transitions. The traditional recurrence quantification analysis fails to detect the latter transitions. Applying our measures to the heart-rate-variability data, we are able to detect and quantify the laminar phases before a life-threatening cardiac arrhythmia occurs thereby facilitating a prediction of such an event. Our findings could be of importance for the therapy of malignant cardiac arrhythmias.

DOI: 10.1103/PhysRevE.66.026702

PACS number(s): 07.05.Kf, 05.45.Tp, 87.80.Tq, 87.19.Hh

**I. INTRODUCTION**

Numerous scientific disciplines, such as astrophysics, biology or geosciences, use data analysis techniques to get an insight into the complex processes observed in nature [1–3], which show generally a nonstationary and complex behavior. As these complex systems are characterized by different transitions between regular, laminar, and chaotic behaviors, the knowledge of these transitions is necessary for understanding the process. However, observational data of these systems are typically rather short. Linear approaches of time series analysis are often not sufficient [4,5] and most of the nonlinear techniques (cf. [6,7]), such as fractal dimensions or Lyapunov exponents [7–10], suffer from the curse of dimensionality and require rather long data series. The uncritical application of these methods, especially to natural data, can therefore be very dangerous and it often leads to serious pitfalls.

To overcome these difficulties other measures of complexity have been proposed, such as the Renyi entropies, the effective measure complexity, the  $\varepsilon$  complexity or the renormalized entropy [11,12]. They are mostly based on symbolic dynamics and are efficient quantities for characterizing measurements of natural systems, such as in cardiology [13–15], cognitive psychology [16] or astrophysics [17–19]. In this paper we focus on another type of measure of complexity, which is based on the method of recurrence plots (RP's). This approach has been introduced for the analysis of nonstationary and rather short data series [20–22]. Moreover, a quantitative analysis of recurrence plots has been proposed to detect typical transitions (e.g., bifurcation points) occurring in complex systems [23–25]. However, the quantities introduced so far are not able to detect more complex transitions, especially chaos-chaos transitions, which are also typical in nonlinear dynamical systems. Therefore in this paper we introduce measures of complexity based on recur-

rence plots, which allow us to identify laminar states and their transitions to regular as well as other chaotic regimes in complex systems. These measures make the investigation of intermittency of processes possible, even if they are only represented by short and nonstationary data series.

The paper is organized as follows. After a short review of the technique of recurrence plots and some measures, we introduce other measures of complexity based on recurrence plots. After that we apply this approach to the logistic equation and demonstrate the ability to detect chaos-chaos transitions. Finally, we apply this technique to heart-rate-variability data [26]. We demonstrate that by applying our proposed methods we are able to detect laminar phases before the onset of a life-threatening cardiac arrhythmia.

**II. RECURRENCE PLOTS AND THEIR QUANTIFICATION**

The method of RP was first introduced to visualize the time dependent behavior of the dynamics of systems, which can be pictured as a trajectory  $\vec{x}_i \in \mathcal{R}^n$  ( $i = 1, \dots, N$ ) in the  $n$ -dimensional phase space [21]. It represents the recurrence of the phase space trajectory to a certain state, which is a fundamental property of deterministic dynamical systems [27,28]. The main step of this visualization is the calculation of the  $N \times N$  matrix,

$$\mathbf{R}_{i,j} := \Theta(\varepsilon_i - \|\vec{x}_i - \vec{x}_j\|), \quad i, j = 1, \dots, N, \quad (1)$$

where  $\varepsilon_i$  is a cutoff distance,  $\|\cdot\|$  is a norm (e.g., the Euclidean norm), and  $\Theta(x)$  is the Heaviside function. The phase space vectors for one-dimensional time series  $u_i$  from observations can be reconstructed by using the Taken's time delay method,  $\vec{x}_i = (u_i, u_{i+\tau}, \dots, u_{i+(m-1)\tau})$  [7]. The dimension  $m$  can be estimated with the method of false nearest neighbors (theoretically,  $m = 2n + 1$ ) [7,27]. The cutoff distance  $\varepsilon_i$  defines a sphere centered at  $\vec{x}_i$ . If  $\vec{x}_j$  falls within this sphere, the state will be close to  $\vec{x}_i$  and thus  $\mathbf{R}_{i,j} = 1$ . These  $\varepsilon_i$  can be either constant for all  $\vec{x}_i$  [22] or they can vary in such a way

\*Electronic address: marwan@agnld.uni-potsdam.de

that the sphere contains a predefined number of close states [21]. In this paper a fixed  $\varepsilon_i$  and the Euclidean norm are used, resulting in a symmetric RP. The binary values in  $R_{i,j}$  can be simply visualized by a matrix plot with the colors black (1) and white (0).

The recurrence plot exhibits characteristic large-scale and small-scale patterns that are caused by typical dynamical behavior [21,24], e.g., diagonals (similar local evolution of different parts of the trajectory) or horizontal and vertical black lines (state does not change for some time).

Zbilut and Webber have recently developed the recurrence quantification analysis (RQA) to quantify an RP [23–25]. They define measures using the recurrence point density and the diagonal structures in the recurrence plot, the *recurrence rate*, the *determinism*, the *maximal length of diagonal structures*, the *entropy*, and the *trend*. A computation of these measures in small windows moving along the main diagonal of the RP yields the time dependent behavior of these variables and, thus, makes the identification of transitions in the time series possible [23].

The RQA measures are mostly based on the distribution of the length of the diagonal structures in the RP. Additional information about further geometrical structures such as vertical and horizontal elements are not included. Gao has therefore recently introduced a recurrence time statistics that corresponds to vertical structures in an RP [29,30]. In the following, we extend this view on the vertical structures and define measures of complexity based on the distribution of the vertical line length. Since we are using symmetric RPs here, we will only consider the vertical structures.

### III. MEASURES OF COMPLEXITY

We consider a point  $\vec{x}_i$  of the trajectory and the set of its associated recurrence points  $S_i := \{\vec{x}_k : \mathbf{R}_{i,k} = 1; k \in [1, \dots, N-1]\}$ . Denote a subset of these recurrence points  $s_i := \{\vec{x}_l \in S_i : (\mathbf{R}_{i,l} \cdot \mathbf{R}_{i,l+1}) + (\mathbf{R}_{i,l} \cdot \mathbf{R}_{i,l-1}) > 0; l \in [1, \dots, N], \mathbf{R}_{i,0} = \mathbf{R}_{i,N+1} = 0\}$ , which contains the recurrence points forming the vertical structures in the RP at column  $i$ . In continuous time systems with high time resolution and with a not too small threshold  $\varepsilon$ , a large part of this set  $s_i$  usually corresponds to the sojourn points described in Refs. [29,30]. Although sojourn points do not occur in maps, the subset  $s_i$  is not necessarily empty. Next, we determine the length  $v$  of all connected subsets  $\{\vec{x}_j \in s_i; \vec{x}_{j+1}, \dots, \vec{x}_{j+v} \in s_i; \vec{x}_{j+v+1} \notin s_i\}$  in  $s_i$ .  $P_i(v) = \{v_l; l = 1, 2, \dots, L\}$  denotes the set of all occurring subset lengths in  $s_i$  and from  $\cup_{i=1}^N P_i(v)$  we determine the distribution of the vertical line lengths  $P(v)$  in the entire RP.

Analogous to the definition of the determinism [24,31], we compute the ratio between the recurrence points forming the vertical structures and the entire set of recurrence points,

$$\Lambda := \frac{\sum_{v=v_{min}}^N v P(v)}{\sum_{v=1}^N v P(v)}, \quad (2)$$

and call it *laminarity*  $\Lambda$ . The computation of  $\Lambda$  is realized for  $v$  that exceeds a minimal length  $v_{min}$ . For maps we use  $v_{min} = 2$ .  $\Lambda$  is the measure of the amount of vertical structures in the whole RP and represents the occurrence of laminar states in the system, without, however, describing the length of these laminar phases. It will decrease if the RP consists of more single recurrence points than vertical structures,

$$T := \frac{\sum_{v=v_{min}}^N v P(v)}{\sum_{v=v_{min}}^N P(v)}, \quad (3)$$

and call it as *trapping time*  $T$ . The computation also uses the minimal length  $v_{min}$  as in  $\Lambda$ . The measure  $T$  contains information about the amount and the length of the vertical structures in the RP.

Finally, we use the maximal length of the vertical structures in the RP,

$$V_{max} = \max(\{v_l; l = 1, 2, \dots, L\}), \quad (4)$$

as a measure that is the analogue to the standard RQA measure  $L_{max}$  [24].

Although the distribution of the diagonal line lengths also contains information about the vertical line lengths, the two distributions are significantly different. In order to compare the measures proposed with the standard RQA measures, we apply them to the logistic map.

### IV. APPLICATION TO THE LOGISTIC MAP

In order to investigate the potentials of  $\Lambda$ ,  $T$ , and  $V_{max}$ , we first analyze the logistic map

$$x_{n+1} = ax_n(1 - x_n), \quad (5)$$

especially the interesting range of the control parameter  $a \in [3.5, 4]$  with a step width of  $\Delta a = 0.0005$ . Starting with the idea of Trulla *et al.* [23] to look for vertical structures, we are especially interested in finding the laminar states in chaos-chaos transitions. Therefore we generate for each control parameter  $a$  a separate time series. In the analyzed range of  $a \in [3.5, 4]$  various regimes and transitions between them occur, e.g., accumulation points, periodic, and chaotic states, band merging points, period doublings, and inner and outer crises [27,32,33].

A useful tool for studying the chaotic behavior is the recursively formed *supertrack functions*

$$s_{i+1}(a) = a s_i(a) [1 - s_i(a)], \quad s_0(a) = \frac{1}{2}, \quad (6)$$

which represent the functional dependence of stable states [33]. The intersection of  $s_i(a)$  with  $s_{i+j}(a)$  indicates the occurrence of a  $j$ -period cycle and the intersection of  $s_i(a)$  with the fixed point  $(1 - 1/a)$  of Eq. (5) indicates the point of an unstable singularity, i.e., laminar behavior (Fig. 1, inter-

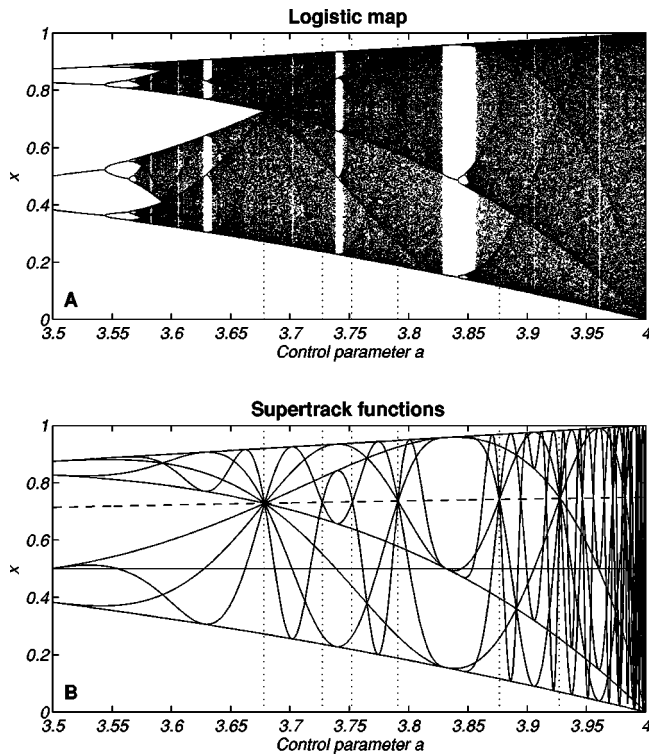


FIG. 1. (a) Bifurcation diagram of the logistic map. (b) Low ordered supertrack functions  $s_i(a)$  ( $i=1, \dots, 10$ ) and the fixed point of the logistic map  $1-1/a$  (dashed). Their intersections represent periodic windows, band merging, and laminar states. The vertical dotted lines show a choosing of points of band merging and laminar behavior ( $a=3.678, 3.727, 3.752, 3.791, 3.877, 3.927$ ).

section points are marked with dotted lines). For each  $a$  we compute a time series of the length  $N=2000$ . In order to exclude transient responses we use the last 1000 values of these data series in the following analysis.

We compute the RP after embedding the time series with a dimension of  $m=1$ , a delay of  $\tau=1$ , and a cutoff distance of  $\varepsilon=0.1$  (in units of the standard deviation  $\sigma$ ). Since the considered example is a one-dimensional map,  $m=1$  is sufficient. In general, a too small embedding leads to false recurrences, that are expressed in numerous vertical structures and diagonals from the upper left corner to the lower right corner [30]. In contrast, an overembedding should theoretically not distort the reconstructed phase trajectory. Whereas false recurrences and overembedding do not strongly influence the measures based on diagonal structures [30], the measures based on vertical structures are, in general, much more sensitive to the embedding. This is due to the fact that the embedding method causes higher-order correlations in the phase-space trajectory, which will be of course visible in the RP. A theoretical and more detailed explanation of this effect within the analysis of RPs is in preparation and beyond the scope of this paper. For the logistic map, however, an increasing of  $m$  slightly amplifies the peaks of the vertical based complexity measures (up to  $m=3$ ), but it does not change the result significantly. The cutoff distance  $\varepsilon$  is selected to be 10% of the diameter of the reconstructed phase space. Smaller values would lead to a better distinction of

small variations (e.g., the range before the accumulation point consists of small variations). However, the recurrence point density decreases in the same way and thus the statistics of continuous structures in the RP soon becomes insufficient. Larger values cause a higher recurrence point density, but a lower sensitivity to small variations.

### A. Recurrence plots of the logistic map

For various values of the control parameter  $a$  we obtain RPs that already exhibit specific features (Fig. 2). Periodic states (e.g., in the periodic window of length 3 at  $a=3.830$ ) cause continuous and periodic diagonal lines in the RP of width of 1. There are no vertical or horizontal lines [Fig. 2(a)]. Band merging points and other cross points of supertrack functions [e.g.,  $a=3.720$ , Fig. 2(c)] represent states with short laminar behavior and cause vertically and horizontally spread black areas in the RP. The band merging at  $a=3.679$  causes frequent laminar states and therefore a lot of vertically and horizontally spread black areas in the RP [Fig. 2(b)]. Fully developed chaotic states ( $a=4$ ) cause a rather homogeneous RP with numerous single points and rare short diagonal or vertical lines [Fig. 2(d)].

### B. Complexity measures of the logistic map

Now we compute the known RQA measures  $\Delta$ ,  $L_{max}$ , and in addition  $\langle L \rangle$  (average length of diagonal lines) and our measures  $\Lambda$ ,  $V_{max}$ , and  $T$  for the entire RP of each control parameter  $a$ . As expected, the known RQA measures  $\Delta$ ,  $L_{max}$ , and  $\langle L \rangle$  clearly detect the transitions from chaotic to periodic sequences and vice versa [Figs. 3(a), 3(c), and 3(e)] [23]. However, it seems that one cannot get more information than the periodic-chaotic/ chaotic-periodic transitions. Near the supertrack crossing points (band merging points included), e.g.,  $a=3.678, 3.791, 3.927$ , there are no significant indications in these RQA measures. They clearly identify the bifurcation points (periodic-chaotic/chaotic-periodic transitions), without, however, finding the chaos-chaos transitions and the laminar states.

Calculating the vertical based measures  $\Lambda$  and  $T$ , we are able to find the periodic-chaotic/ chaotic-periodic transitions and the laminar states [Figs. 3(b) and 3(f)]. The occurrence of vertical lines starts shortly before the band merging from two to one band at  $a=3.678 \dots$

For smaller  $a$  values the consecutive points jump between the two bands and it is therefore impossible to obtain a laminar behavior. A longer persistence of states is not possible until all bands are merged. However, due to the finite range of neighborhood searching in the phase space, vertical lines occur before this point.

Vertical lines occur much more frequently at supertrack crossing points (band merging points included) than in other chaotic regimes, which is revealed by  $\Lambda$  [cf. Fig. 3(b), again, supertrack crossing points are marked with dotted lines]. As in the states before the merging from two to one band, vertical lines are not found within periodic windows, e.g.,  $a=3.848$ . The mean of the distribution of  $v$  is the introduced measure  $T$  [Fig. 3(f)]. It will vanish if  $a$  is smaller than the point of merging from two to one band.  $T$  increases at those

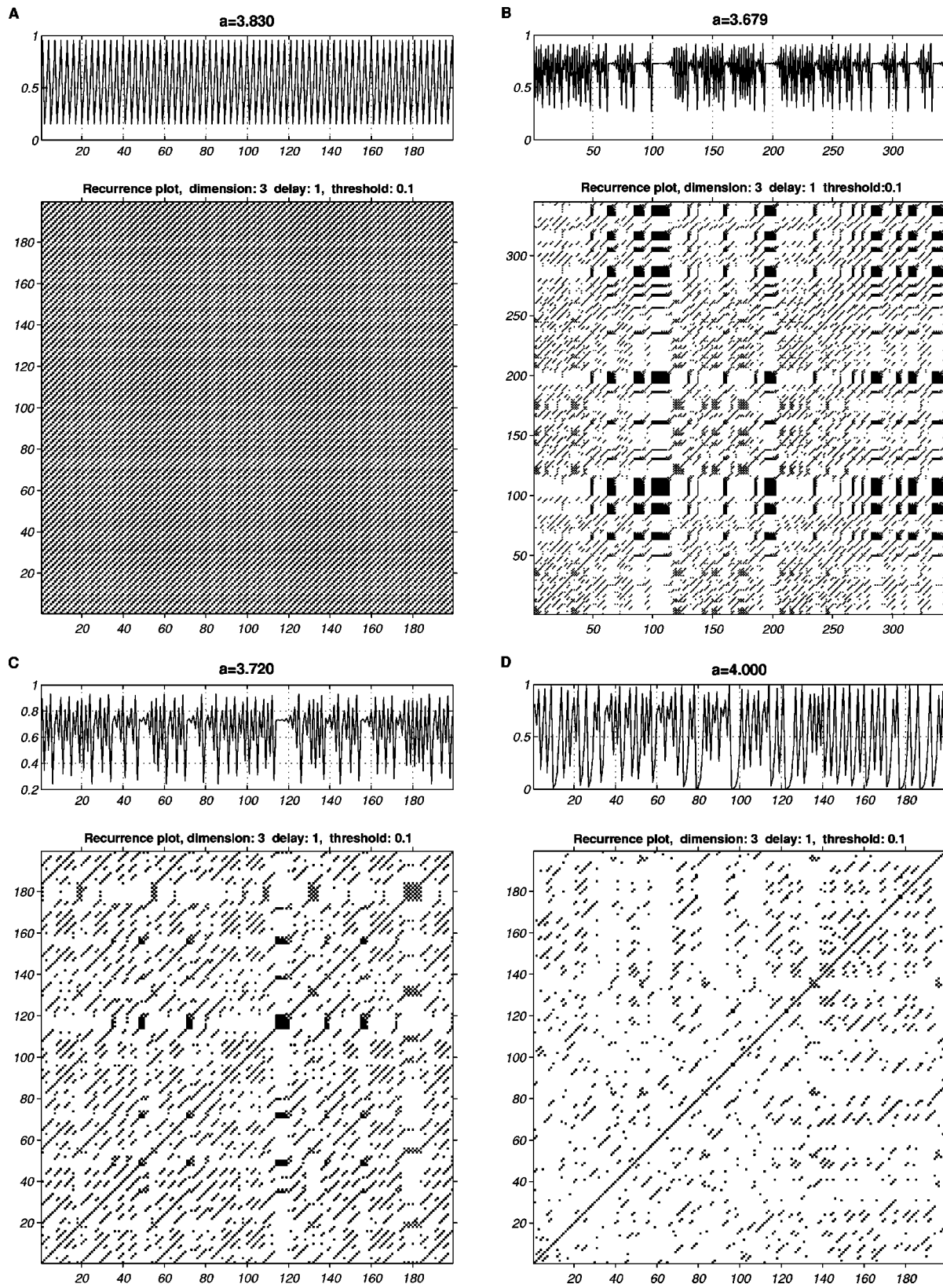


FIG. 2. Recurrence plots (RPs) of the logistic map for various control parameters  $a$ , near different qualitative changes: 3-period window  $a=3.830$  (a); band merging  $a=3.679$  (b); supertrack intersection  $a=3.720$  (c); and chaos (exterior crisis)  $a=4$  (d), with embedding dimension  $m=1$ , time delay  $\tau=1$ , and distance cutoff  $\varepsilon=0.1\sigma$ .

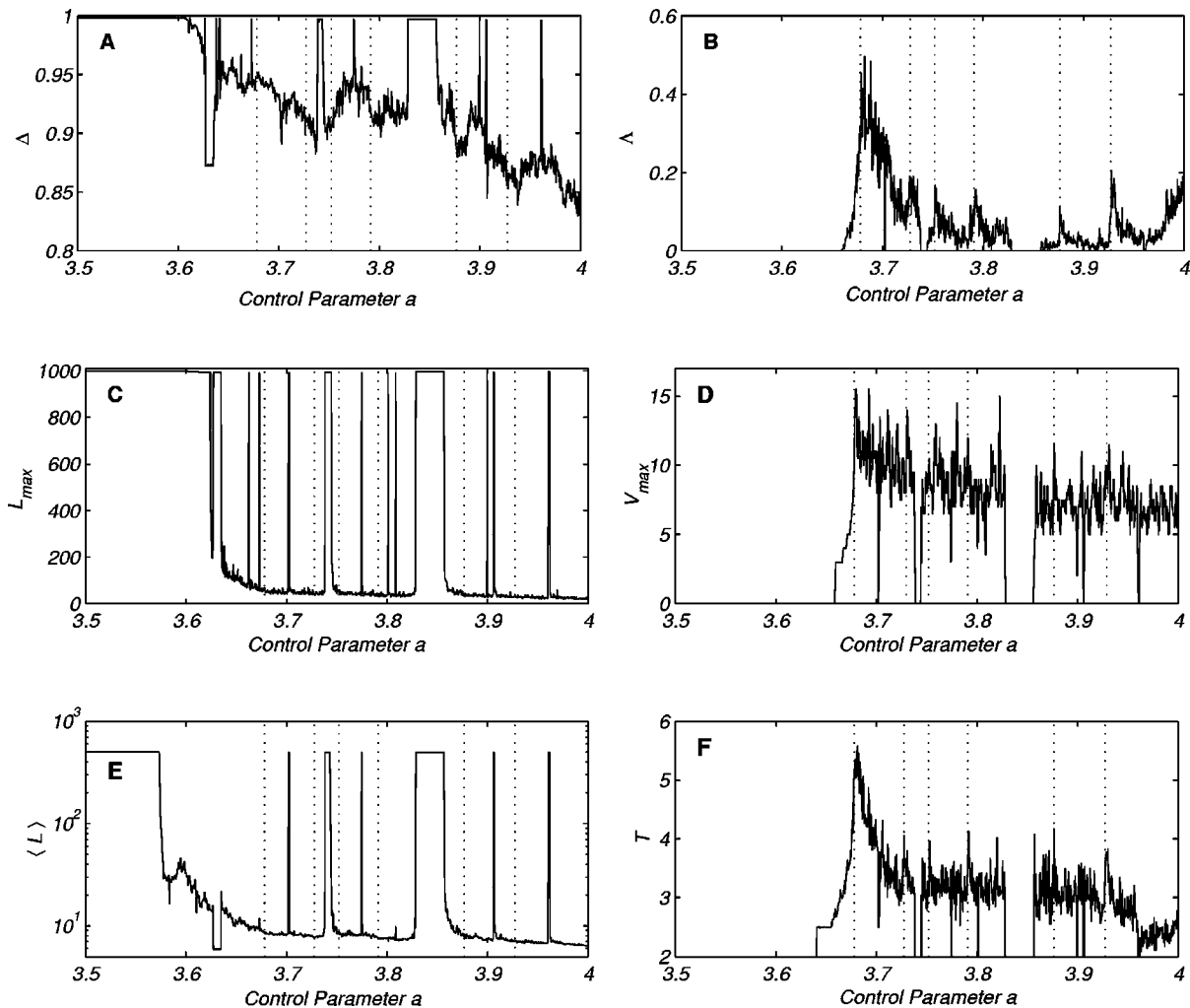


FIG. 3. Selected RQA parameters  $\Delta$ ,  $L_{max}$ , and  $\langle L \rangle$  and the measures  $\Lambda$ ,  $V_{max}$ , and  $T$ . The vertical dotted lines show some of the points of band merging and laminar behavior (cf. Fig. 1), whereby not all of them have been marked. Whereas  $\Delta$  (a),  $L_{max}$  (c), and  $\langle L \rangle$  (e) show periodic-chaotic/ chaotic-periodic transitions (maxima),  $\Lambda$  (b),  $V_{max}$  (d), and  $T$  (f) exhibit in addition to those transitions (minima) chaotic-chaotic transitions (maxima). The differences between  $\Delta$  and  $V_{max}$  are caused by the fact that  $\Delta$  measures only the amount of laminar states, whereas  $V_{max}$  measures the maximal duration of the laminar states. Although some peaks of  $V_{max}$  and  $T$  are not at the dotted lines, they correspond to laminar states (not all can be marked).

points where more low ordered supertrack functions are crossing [Fig. 3(f)]. This corresponds to the occurrence of laminar states. Although  $V_{max}$  also reveals laminar states, it is quite different from the other two measures, because it gives the maximum of all of the durations of the laminar states. However, periodic states are also associated with vanishing  $T$  and  $V_{max}$ . Hence, the vertical length based measures yield periodic-chaotic/chaotic-periodic as well as chaos-chaos transitions (laminar states).

We have also computed  $\Lambda$ ,  $V_{max}$ , and  $T$  for the logistic map with transients using the same approach as described in [23]. The qualitative statement of the measures is the same as above.

## V. APPLICATION TO HEART-RATE-VARIABILITY DATA

Heart-rate variability (HRV) typically shows a complex behavior and it is difficult to identify disease specific patterns [34]. A fundamental challenge in cardiology is to find early

signs of ventricular tachyarrhythmias (VT) in patients with an implanted cardioverter-defibrillator (ICD) based on HRV data [26,35–37]. Therefore standard HRV parameters from time and frequency domains [38], parameters from symbolic dynamics [13,14] as well as the finite-time growth rates [39] were applied to the data of a clinical pilot study [26]. Using two nonlinear approaches, we have recently found significant differences between control and VT time series based mainly on laminar phases in the data before a VT. Therefore the aim of this investigation is to test whether our RP approach is suitable to identify and quantify these laminar phases.

The defibrillators used in the study cited (PCD 7220/7221, Medtronic) are able to store at least 1000 beat-to-beat intervals prior to the onset of VT (10-ms resolution), corresponding to approximately 9–15 min. We reanalyze these intervals from 17 chronic heart failure ICD patients just before the onset of a VT and at a control time, i.e., without a following arrhythmic event. Time series including more than

TABLE I. Results of maximal diagonal and vertical line length shortly before VT and at control time, and nonparametric Mann-Whitney  $U$ -test:  $p$  represents significance; \* is for  $p < 0.05$ ; \*\* for  $p < 0.01$ ; ns for not significant,  $p \geq 0.05$ .

$m$	$\varepsilon$	VT	Control	$p$
Maximal diagonal line length $L_{max}$				
3	77	$396.6 \pm 253.8$	$261.5 \pm 156.6$	ns
6	110	$447.6 \pm 269.1$	$285.5 \pm 160.4$	*
9	150	$504.6 \pm 265.9$	$311.6 \pm 157.2$	*
12	170	$520.7 \pm 268.8$	$324.7 \pm 180.2$	*
Maximal vertical line length $V_{max}$				
3	77	$261.4 \pm 193.5$	$169.2 \pm 135.9$	*
6	110	$283.7 \pm 190.4$	$179.5 \pm 134.1$	**
9	150	$342.4 \pm 193.6$	$216.1 \pm 137.1$	**
12	170	$353.5 \pm 221.4$	$215.1 \pm 138.6$	**

one nonsustained VT, with induced VTs, pacemaker activity or more than 10% of ventricular premature beats are not considered in this analysis. Some patients had several VTs; we finally had 24 time series with a subsequent VT and the respective 24 control series without a life-threatening arrhythmia. In order to analyze only the dynamics occurring

just before a VT, the beat-to-beat intervals of the VT itself at the end of the time series are removed from the tachograms.

We calculate all standard RQA parameters described in Ref. [24] as well as the measures laminarity  $\Lambda$ , trapping time  $T$ , and maximal vertical line length  $V_{max}$  (similar to the maximal diagonal line length  $L_{max}$ ) for different embedding dimensions  $m$  and nearest neighboring radii  $\varepsilon$ . We find differences between both groups of data for several of the parameters mentioned above. However, the most significant parameters are  $V_{max}$  and  $L_{max}$  for rather large radii (Table I). The vertical line length  $V_{max}$  is more powerful in discriminating both groups than the diagonal line length  $L_{max}$ , as can be recognized by the higher  $p$  values for  $V_{max}$  (Table I). Figure 4 gives a typical example of the recurrence plots before a VT and at a control time with an embedding of 6 and a radius of 110. The RP before a life-threatening arrhythmia is characterized by large black rectangles ( $V_{max} = 242$  here), whereas the RP from the control series shows only small rectangles ( $V_{max} = 117$ ).

## VI. SUMMARY

We have introduced three more RPs based measures of complexity, the laminarity  $\Lambda$ , the trapping time  $T$ , and the maximal length of vertical structures in the RP,  $V_{max}$ . These

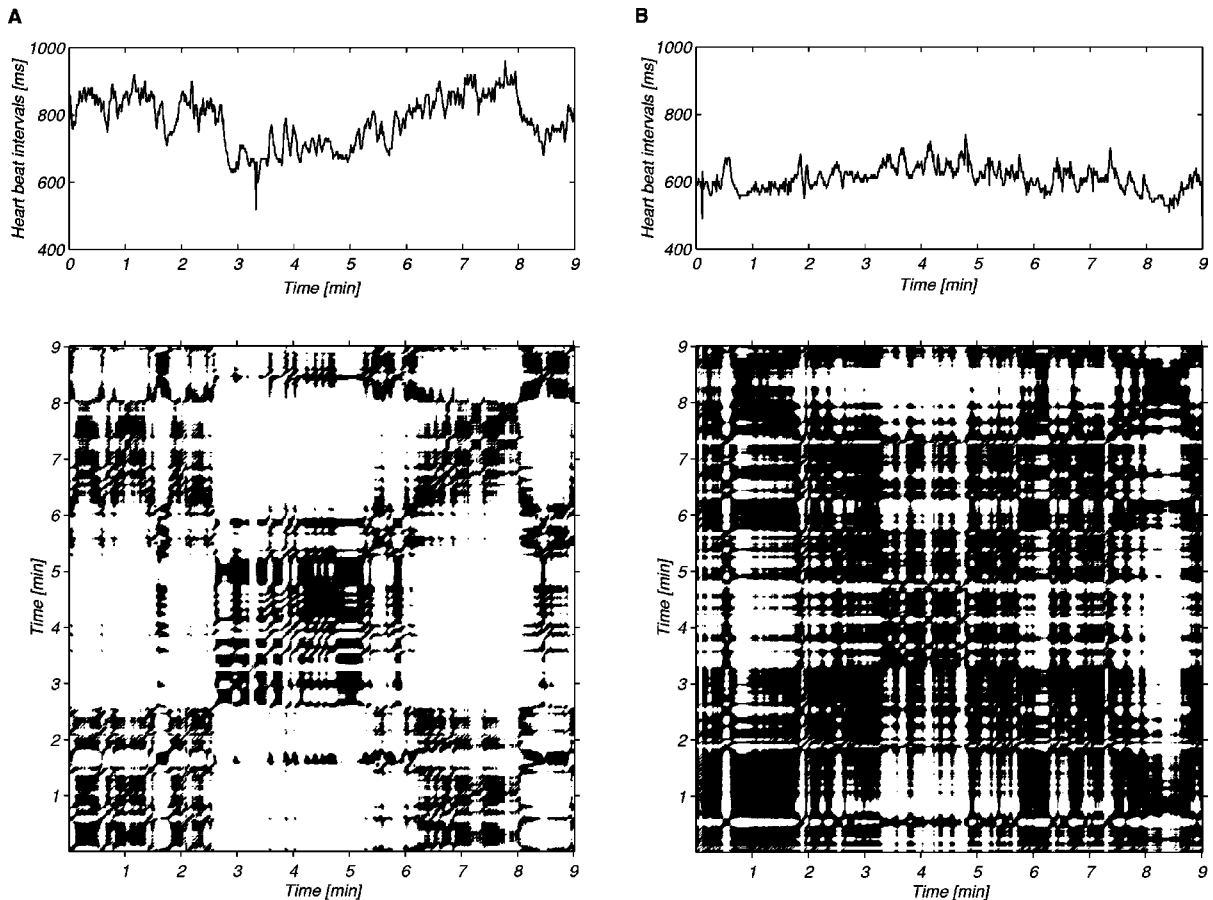


FIG. 4. Recurrence plots of the heart beat interval time series at a control time (a) and before a VT (b) with an embedding of 6 and a radius of 110. The RP before a life-threatening arrhythmia is characterized by big black rectangles, whereas the RP from the control series shows only small rectangles.

measures of complexity have been applied to the logistic map and heart-rate-variability data. In contrast to the known RQA measures [23,25], that are able to detect transitions between chaotic and periodic states (and vice versa), our measures enable us to identify laminar states too, i.e., chaos-chaos transitions. These measures are provided by the vertical lines in recurrence plots. The occurrence of vertical (and horizontal) structures is directly related to the occurrence of laminar states.

The laminarity  $\Lambda$  enables us generally to detect laminar states in a dynamical system. The trapping time  $T$  contains information about the frequency of the laminar states and their lengths. The maximal length  $V_{max}$  reveals information about the time duration of the laminar states thus making the investigation of intermittency possible.

If the embedding of the data is too small, it will lead to false recurrences, which is expressed in numerous vertical structures and diagonals perpendicular to the main diagonal. Whereas false recurrences do not influence the measures based on diagonal structures, the measures based on vertical structures are sensitive to it.

The application of these measures to the logistic equation for a range of various control parameters has revealed points of laminar states without any additional knowledge about the characteristic parameters or dynamical behavior of the specific systems. Nevertheless,  $\Lambda$ ,  $V_{max}$ , and  $T$  are different in their magnitudes. Further investigations are necessary to understand all relations between the magnitudes of  $V_{max}$  and the recognized chaos-chaos transitions.

The application of these complexity measures to the ICD

stored heart-rate data before the onset of a life-threatening arrhythmia seems to be very successful for the detection of laminar phases thus making a prediction of such VT possible. The differences between the VT and the control series are more significant than in Ref. [26]. However, two limitations of this study are the relatively small number of time series and the reduced statistical analysis (no subdivisions concerning age, sex, and heart disease). For this reason, our results should be validated on a larger database. Furthermore, this investigation could be enhanced for tachograms including more than 10% ventricular premature beats. In conclusion, this study has demonstrated that the RQA based complexity measures could play an important role in the prediction of VT events even in short term HRV time series.

Many biological data contain epochs of laminar states, which can be detected and quantified by the RP based measures. We have demonstrated differences between the measures based on the vertical and the diagonal structures and therefore we suggest the use of the method proposed in this paper in addition to the traditional measures.

A download of the Matlab implementation is available at [www.agnld.uni-potsdam.de/~marwan](http://www.agnld.uni-potsdam.de/~marwan)

#### ACKNOWLEDGMENTS

This work was partly supported by the priority program SPP 1097 of the German Science Foundation (DFG). We gratefully acknowledge M. Romano, M. Thiel, and U. Schwarz for fruitful discussions.

- 
- [1] L. Glass, *Nature (London)* **410**, 277 (2001).
  - [2] B. Blasius, A. Huppert, and L. Stone, *Nature (London)* **399**, 354 (1999).
  - [3] K. B. Marvel, *Nature (London)* **411**, 252 (2001).
  - [4] A. L. Goldberger, D. R. Rigney, J. Mietus, E. M. Antman, and S. Greenwald, *Experientia* **44**, 983 (1988).
  - [5] L. Glass and D. Kaplan, *Med. Prog. Technol.* **19**, 115 (1993).
  - [6] H. D. I. Abarbanel, R. Brown, J. J. Sidorowich, and L. S. Tsimring, *Rev. Mod. Phys.* **65**, 1331 (1993).
  - [7] H. Kantz and T. Schreiber, *Nonlinear Time Series Analysis* (Cambridge University Press, Cambridge, England, 1997).
  - [8] J. Kurths and H. Herzel, *Physica D* **25**, 165 (1987).
  - [9] B. B. Mandelbrot, *The Fractal Geometry of Nature* (Freeman, San Francisco, 1982).
  - [10] A. Wolf, J. B. Swift, H. L. Swinney, and J. A. Vastano, *Physica D* **16**, 285 (1985).
  - [11] R. Wackerbauer, A. Witt, H. Atmanspacher, J. Kurths, and H. Scheingraber, *Chaos, Solitons Fractals* **4**, 133 (1994).
  - [12] P. E. Rapp, C. J. Cellucci, K. E. Korslund, T. A. Watanabe, and M. A. Jimenez-Montano, *Phys. Rev. E* **64**, 016209 (2001).
  - [13] J. Kurths, A. Voss, A. Witt, P. Saparin, H. J. Kleiner, and N. Wessel, *Chaos* **5**, 88 (1995).
  - [14] A. Voss, J. Kurths, H. J. Kleiner, A. Witt, N. Wessel, P. Saparin, K. J. Osterziel, R. Schurath, and R. Dietz, *Cardiovasc. Res.* **31**, 419 (1996).
  - [15] N. Wessel, A. Voss, J. Kurths, A. Schirdewan, K. Hnatkova, and M. Malik, *Med. Biol. Eng. Comput.* **38**, 680 (2000).
  - [16] R. Engbert, M. S. C. Scheffczyk, J. Kurths, R. Krampe, R. Kliegl, and F. Drepper, *Nonlin. Anal. Theor. Meth. Appl.* **30**, 973 (1997).
  - [17] A. Hempelmann and J. Kurths, *Astron. Astrophys.* **232**, 356 (1990).
  - [18] U. Schwarz, A. O. Benz, J. Kurths, and A. Witt, *Astron. Astrophys.* **277**, 215 (1993).
  - [19] A. Witt, J. Kurths, F. Krause, and K. Fischer, *Geophys. Astrophys. Fluid Dyn.* **77**, 79 (1994).
  - [20] M. C. Casdagli, *Physica D* **108**, 12 (1997).
  - [21] J.-P. Eckmann, S. O. Kamphorst, and D. Ruelle, *Europhys. Lett.* **5**, 973 (1987).
  - [22] M. Koebe and G. Mayer-Kress, in *Proceedings of SFI Studies in the Science of Complexity. Nonlinear Modeling and Forecasting*, edited by M. Casdagli and S. Eubank (Addison-Wesley, Redwood City, CA, 1992), Vol. XXI, pp. 361–378.
  - [23] L. L. Trulla, A. Giuliani, J. P. Zbilut, and C. L. Webber, Jr., *Phys. Lett. A* **223**, 255 (1996).
  - [24] C. L. Webber, Jr., and J. P. Zbilut, *J. Appl. Physiol.* **76**, 965 (1994).
  - [25] J. P. Zbilut and C. L. Webber Jr., *Phys. Lett. A* **171**, 199 (1992).
  - [26] N. Wessel, C. Ziehmann, J. Kurths, U. Meyerfeldt, A. Schirdewan, and A. Voss, *Phys. Rev. E* **61**, 733 (2000).

- [27] J. H. Argyris, G. Faust, and M. Haase, *An Exploration of Chaos* (North-Holland, Amsterdam, 1994).
- [28] E. Ott, *Chaos in Dynamical Systems* (Cambridge University Press, Cambridge, 1993).
- [29] J. B. Gao, Phys. Rev. A **83**, 3178 (1999).
- [30] J. B. Gao and H. Q. Cai, Phys. Lett. A **270**, 75 (2000).
- [31] N. Marwan, Master's thesis, Dresden University of Technology, Dresden, 1999.
- [32] P. Collet and J.-P. Eckmann, *Iterated Maps on the Interval as Dynamical Systems* (Birkhäuser, Basel, 1980).
- [33] E. M. Oblow, Phys. Lett. A **128**, 406 (1988).
- [34] A. Schumann, N. Wessel, A. Schirdewan, K. J. Osterziel, and A. Voss, Stat. Med. (to be published).
- [35] J. O. Diaz, T. H. Makikallio, H. V. Huikuri, G. Lopera, R. D. Mitrani, A. Castellanos, R. J. Myerburg, L. P. Roza, F. Pava, and C. A. Morillo, Am. J. Cardiol. **87**, 1123 (2001).
- [36] H. V. Huikuri and T. H. Makikallio, Auton. Neurosci. **90**, 95 (2001).
- [37] S. Guzzetti, R. Magatelli, E. Borroni, and S. Mezzetti, Auton. Neurosci. **90**, 102 (2001).
- [38] Task Force of the European Society of Cardiology and the North American Society of Pacing and Electrophysiology, Circulation **93**, 1043 (1996).
- [39] J. M. Nese, Physica D **35**, 237 (1989).